

Structural length-scale of β relaxation in metallic glass

Cite as: J. Chem. Phys. **157**, 184504 (2022); <https://doi.org/10.1063/5.0123202>

Submitted: 29 August 2022 • Accepted: 24 October 2022 • Accepted Manuscript Online: 24 October 2022 • Published Online: 10 November 2022

 Qun Yang, Shuai Wei, Yang Yu, et al.



View Online



Export Citation



CrossMark

ARTICLES YOU MAY BE INTERESTED IN

[Understanding the difference in the stretched structural relaxations probed by dielectric and enthalpic studies of glass forming substances](#)

The Journal of Chemical Physics **157**, 184501 (2022); <https://doi.org/10.1063/5.0122186>

[Molecular-based analysis of nanoparticle solvation: Classical density functional approach](#)

The Journal of Chemical Physics **157**, 184505 (2022); <https://doi.org/10.1063/5.0128817>

[Manifestations of the structural origin of supercooled water's anomalies in the heterogeneous relaxation on the potential energy landscape](#)

The Journal of Chemical Physics **157**, 184503 (2022); <https://doi.org/10.1063/5.0124041>



Special Topics Open for Submissions

[Learn More](#)

Structural length-scale of β relaxation in metallic glass

Cite as: J. Chem. Phys. 157, 184504 (2022); doi: 10.1063/5.0123202

Submitted: 29 August 2022 • Accepted: 24 October 2022 •

Published Online: 10 November 2022



Qun Yang,¹ Shuai Wei,^{2,3} Yang Yu,¹ Hui-Ru Zhang,¹ Liang Gao,¹ Qing-Zhou Bu,¹ Narges Amini,² Yu-Dong Cheng,⁴ Fan Yang,⁵ Alexander Schoekel,⁶ and Hai-Bin Yu^{1,a)}

AFFILIATIONS

¹ Wuhan National High Magnetic Field Center and School of Physics, Huazhong University of Science and Technology, Wuhan 430074, Hubei, China

² Department of Chemistry, Aarhus University, 8000 Aarhus, Denmark

³ iMAT Centre for Integrated Materials Research, Aarhus University, Aarhus, Denmark

⁴ Center for Alloy Innovation and Design, State Key Laboratory for Mechanical Behavior of Materials, Xi'an Jiaotong University, Xi'an 710061, China

⁵ Institut für Materialphysik im Weltraum, Deutsches Zentrum für Luft- und Raumfahrt (DLR), 51170 Köln, Germany

⁶ Deutsches Elektronen-Synchrotron DESY, 22607 Hamburg, Germany

^{a)} Author to whom correspondence should be addressed: haibinyu@hust.edu.cn

ABSTRACT

Establishing the structure–property relationship is an important goal of glassy materials, but it is usually impeded by their disordered structure and non-equilibrium nature. Recent studies have illustrated that secondary (β) relaxation is closely correlated with several properties in a range of glassy materials. However, it has been challenging to identify the pertinent structural features that govern it. In this work, we show that the so-called polyamorphous transition in metallic glasses offers an opportunity to distinguish the structural length scale of β relaxation. We find that, while the glass transition temperature and medium-range orders (MROs) change rapidly across the polyamorphous transition, the intensity of β relaxation and the short-range orders (SROs) evolve in a way similar to those in an ordinary reference glass without polyamorphous transition. Our findings suggest that the MRO accounts mainly for the global stiffening of the materials and the glass transition, while the SRO contributes more to β relaxation *per se*.

Published under an exclusive license by AIP Publishing. <https://doi.org/10.1063/5.0123202>

Glass represents a unique state of matter, wherein the distinction between solid and liquid structures is diminished. The absence of long-range atomic order in glass leads to numerous possible configurational arrangements, as opposed to a limited few for the crystalline counterparts, thus featuring diverse dynamic processes, denoted as relaxations, over a wide range of temperature and time scales.^{1–7} Among others, a so-called Johari–Goldstein (or secondary β) relaxation has received considerable attention in recent decades.^{2,7} It has been observed in a wide variety of glassy materials, such as molecular,^{8–12} oligomeric,¹³ polymeric,^{14–16} ionic,^{17,18} metallic,^{7,19,20} and chalcogenide glasses.²¹ In some glassy materials, it manifests as a pronounced peak, as probed by dielectric or mechanical spectra, while in some other materials it behaves as the so-called excess wing.^{8–12}

Remarkably, several important properties of glasses were revealed, as correlating to β relaxations. For example, mechanical ductility has been linked to the presence of β relaxations near or below room temperature in polymers²⁰ and metallic glasses (MGs).^{7,19,22} Functional properties, such as the decoloration kinetics of photochromic dyes in co-polycarbonates¹⁴ and the soft magnetic properties of MGs have also been proposed to be related to β relaxation.²³ Recently, Peng *et al.* reported that β relaxation might play a role in facilitating the crystallization of amorphous phase-change materials, which are the basis of non-volatile, phase-change memory devices.²¹ By considering the characteristics of β relaxation as a strategy, Qian *et al.* designed polymers with a low dielectric constant and loss for high-frequency electronic circuits used in 5G wireless networks.²⁴ The studies of their underlying mechanism suggested

that the β relaxation acts as a kind of “flow unit” that allows atoms to rearrange in the seemingly rigid glass.

From the glass-transition perspective, accumulating evidence has suggested that the (de)vitrification kinetics are not driven by the structural α relaxation alone, as conventionally thought.^{2,25,26} Instead, β relaxation must also play a role in reducing the activation energy barrier and facilitating atomic dynamics.^{20,27,28}

Despite its technological relevance and theoretical significance, the structural origin of the β relaxation has not been established and represents an example of the long-standing challenge in glass materials and physics, that is, to predict the dynamics of glass from its static structures. In particular, the characteristic structural length scale for β relaxation is still under debate. It is a prerequisite to identify the pertinent structural length scale for a fundamental understanding of the origin of the β relaxation. Even so, such a length scale has been estimated to range from very local (the first atomic shell) to quite extended (approximately tens of nanometers) based on different investigations.^{29–35} Table S1 (see the [supplementary material](#)) summarizes the reported structural length scale of β relaxation in MGs known at present, which is compared with molecular glasses.^{36–41}

One major obstacle to overcome is the difficulty in controlling and probing the disordered structures of glasses to allow a systematic change in the β relaxation as a function of structural length scales. The short- and medium-range structures usually change in a coupled way in most model systems in experiments, which are further entangled with the effects of different chemical compositions. Coming to the rescue are the recently discovered polyamorphous transitions, which refer to the phenomenon wherein one amorphous substance can transform between two or more distinct amorphous phases with different properties in the same composition.^{42–45} According to the two-order-parameter model,⁴⁵ these amorphous phases have different structures, configurational entropy, and relaxation dynamics.^{46–53} Hence, they might serve as ideal model systems to provide crucial information on these poorly understood problems if structural changes can be finely controlled in the same chemical composition.

In this work, we investigate the β relaxation in a $\text{La}_{65}\text{Co}_{25}\text{Al}_{10}$ MG with a polyamorphous transition in the supercooled liquid region and compare it with that in an ordinary $\text{La}_{50}\text{Ni}_{35}\text{Al}_{15}$ MG. Both of them have pronounced β relaxation peaks, which facilitate the discernment of their different behaviors. Figure 1(a) shows the heat flow curve of the as-cast $\text{La}_{65}\text{Co}_{25}\text{Al}_{10}$ MG measured by a differential scanning calorimeter (DSC). It has a glass transition temperature $T_g \sim 432$ K followed by a heat-releasing peak at ~ 469 K. As demonstrated by Lou *et al.*⁴⁶ for the same MG and Shen *et al.*⁴⁷ for a similar composition, this peak is not due to the crystallization of the glass, but to a polyamorphous transition instead. By cooling the heated sample from $T_a = 493$ K (the finishing temperature of the transition peak) at a rate of 3 K/min, we obtained a sample that had experienced a polyamorphous transition (denoted as PT-MG). The controlled temperature program in which the samples were heat-treated by a dynamical mechanical analyzer (DMA) is shown in the [supplementary material](#) (Fig. S1). We verified that our samples remained amorphous ([supplementary material](#) Fig. S2). Figure 1(a) also shows the heat flow curve of the PT-MG. We find that the heat-releasing peak at ~ 469 K disappears, and a new glass transition at $T_g \sim 485$ K can be observed. Thus, the T_g increases by 53 K,

which suggests higher kinetic stability of PT-MG.^{51,54,55} Furthermore, the phenomenon of an enhanced glass transition temperature for $\text{La}_{65}\text{Co}_{25}\text{Al}_{10}$ MG after the polyamorphous transition was also confirmed by temperature-modulated DSC (TMDSC) experiments (see Fig. S3 of the [supplementary material](#)).

Figure 1(b) presents the damping factor $\tan \delta$ as a function of the temperature of the as-cast MG and PT-MG for $\text{La}_{65}\text{Co}_{25}\text{Al}_{10}$, measured at a frequency of $f = 1$ Hz. The intensity and peak temperature of the β relaxation of PT-MG change compared significantly with those of the as-cast sample. Quantitatively, the peak intensity of β relaxation is suppressed from $\tan \delta = 0.041$ for the as-cast state to $\tan \delta = 0.013$ for PT-MG. The latter corresponds to a factor of 0.32 of the former. Meanwhile, the peak position of β relaxation increases from $T_\beta = 331$ K for the as-cast state to $T_\beta = 383$ K for PT-MG. Thus, the peak temperature increases by 52 K for the β relaxation. This change is remarkable, considering that, in the absence of chemical composition changes, physical methods can only slightly increase the temperature of the β relaxation peak.

For comparison, we performed similar experiments on an ordinary reference ($\text{La}_{50}\text{Ni}_{35}\text{Al}_{15}$) MG without a polyamorphous transition. Similar to $\text{La}_{65}\text{Co}_{25}\text{Al}_{10}$, we prepared two samples: one sample was the as-cast, and the other was pretreated by heating to $T_a = 473$ K before subsequent cooling to room temperature. As shown in Fig. 1(c), the DSC curves indicate that there is a change only in the relaxation enthalpy due to structural relaxation, while T_g remains almost unchanged. From dynamic mechanical spectroscopy, as shown in Fig. 1(d), we find that the intensity of the β relaxation of $\text{La}_{50}\text{Ni}_{35}\text{Al}_{15}$ MG decreases from $\tan \delta = 0.033$ to 0.0165, which corresponds to a factor of 0.5. Notably, the characteristic temperature of the β relaxation increases slightly by only 9 K, which is in sharp contrast to the increase of 52 K for the $\text{La}_{65}\text{Co}_{25}\text{Al}_{10}$ MG that has a polyamorphous transition.

We next progressively vary the finishing temperature T_a of the first heating to systematically study how the annealing and the polyamorphous transition influence the evolution of the β relaxation. This protocol is meant to separate the different effects of aging and polyamorphous transition, as both might have played a role.

Figures 2(a) and 2(b), show a three-dimensional curve plot and a two-dimensional map of the damping factor $\tan \delta$ curves of $\text{La}_{65}\text{Co}_{25}\text{Al}_{10}$ MG that were heat-treated at different T_a , measured at a frequency $f = 1$ Hz, respectively. We find that the intensity of the β relaxation peak decreases monotonously in all the studied T_a temperature ranges. On the other hand, the characteristic temperature of the β relaxation peak first changes very little when $T_a < 440$ K, but it increases considerably after that temperature. We have verified that other frequencies (between 0.5 and 32 Hz, accessible by mechanical spectroscopy) give the similar results.

Similarly, Figs. 2(c) and 2(d) display the temperature-dependent $\tan \delta$ under different T_a values for the reference $\text{La}_{50}\text{Ni}_{35}\text{Al}_{15}$ MG. We find that the intensity of the β relaxation peak gradually decreases in a manner similar to that of $\text{La}_{65}\text{Co}_{25}\text{Al}_{10}$ MG. However, the characteristic temperature of β relaxation, T_β , increases only slightly. This mimics the T_β behavior of $\text{La}_{65}\text{Co}_{25}\text{Al}_{10}$ before the polyamorphous transition occurs, but not after that.

We next show quantitative comparisons between them in Figs. 2(e) and 2(f). Figure 2(e) shows $\Delta T_\beta = T_{\beta@T_a} - T_{\beta@as-cast}$ as a function of T_a for the two MGs. As outlined above, it demonstrates a clear difference: $\text{La}_{65}\text{Co}_{25}\text{Al}_{10}$ (which has a polyamorphous

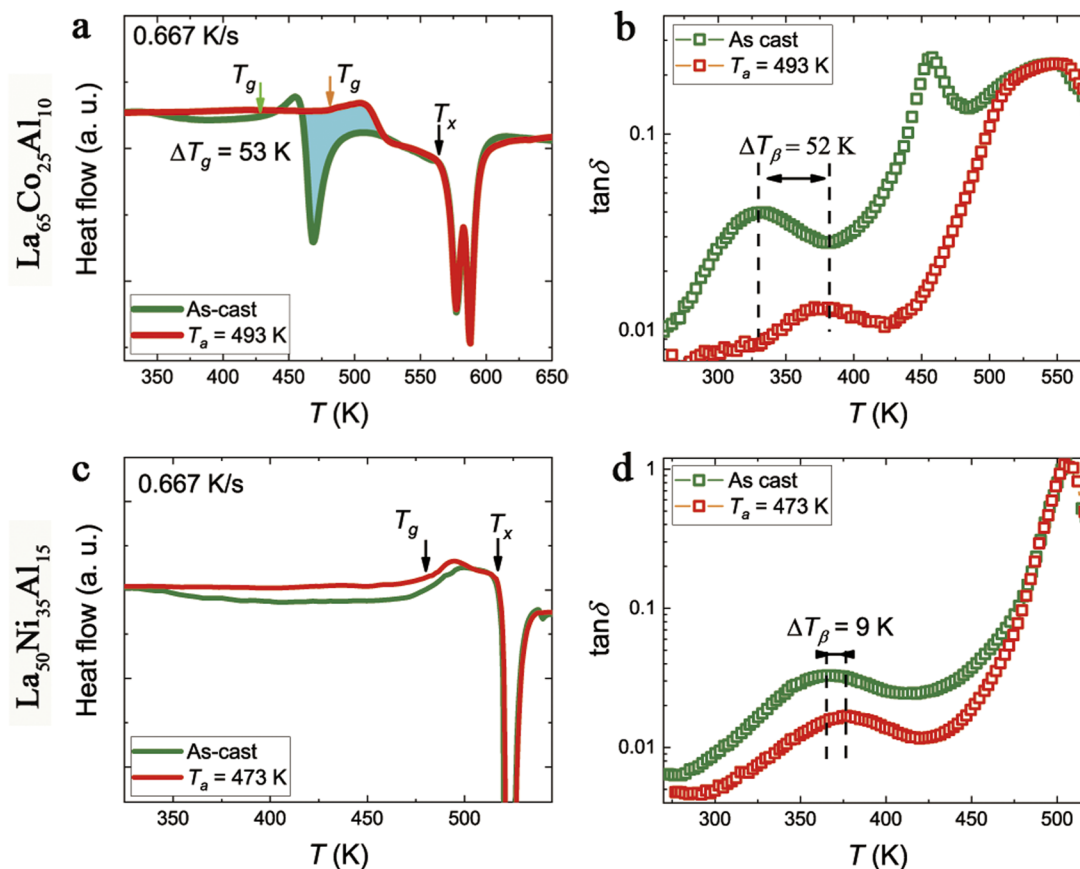


FIG. 1. (a) DSC heat flow curves of the as-cast and PT samples (after polymorphous transition) of $\text{La}_{65}\text{Co}_{25}\text{Al}_{10}$ MG, measured with a heating rate of 40 K/min. (b) Temperature dependence of the damping factor $\tan \delta$ of the as-cast and PT $\text{La}_{65}\text{Co}_{25}\text{Al}_{10}$ MG, measured at a frequency of 1 Hz. (c) Comparison of heat flow curves of as-cast and pre-treated samples for $\text{La}_{50}\text{Ni}_{35}\text{Al}_{15}$ MG (40 K/min). (d) Correspondingly, the change of the β relaxation peak of $\text{La}_{50}\text{Ni}_{35}\text{Al}_{15}$ MG before and after pre-treated (1 Hz).

transition) shows a substantially larger ΔT_β with a maximum value of 52 K, while for ordinary MG, ΔT_β is below 10 K in the full temperature range. Moreover, the abrupt increase in T_β takes place in the range 450 to 500 K, which coincides with the temperature range of the polymorphous transition. These results suggest that the dramatic increase in ΔT_β in $\text{La}_{65}\text{Co}_{25}\text{Al}_{10}$ is not due to structural aging, but results from the underlying polymorphous transition.

Figure 2(f) compares the evolution of the magnitude of the β relaxation peak for the two MGs. For this purpose, we define $\Delta \tan \delta / \tan \delta_{\text{as-cast}}$, where $\Delta \tan \delta = \tan \delta_{\text{as-cast}} - \tan \delta_{T_a}$, to characterize how large the fraction of the β relaxation is reduced. One can see that the two MGs show almost the same behavior. This implies that the suppression of β relaxation is mainly attributed to the effects of aging, while the polymorphous transition contributes marginally to the suppression of β relaxation intensity. Therefore, the polymorphous transition mainly influences the peak temperature, but not the intensity of the β relaxation of MGs.

Figure 2(g) shows the storage modulus E' of the $\text{La}_{65}\text{Co}_{25}\text{Al}_{10}$ and $\text{La}_{50}\text{Ni}_{35}\text{Al}_{15}$ MGs as a function of temperature, measured with a frequency $f = 1$ Hz, upon heating from room temperature. For the

ordinary MG ($\text{La}_{50}\text{Ni}_{35}\text{Al}_{15}$), E' drops sharply when the primary (α) relaxation is approached, which suggests a glass softening process. On the other hand, for $\text{La}_{65}\text{Co}_{25}\text{Al}_{10}$, the drop in E' around the α relaxation is small because the polymorphous transition takes place soon after the α relaxation, and the polymorphous transition is a structural ordering process that competes with the α relaxation; thus, the glass stiffens again.

Why does the characteristic temperature of β relaxation in the polyamorphous MG increase so much higher than that in ordinary MGs? Figure 1 shows that PT-MG also exhibits an enhanced glass transition temperature T_g . This implies a possible connection between them. We validated this correlation using Fig. 3, which plots T_β against T_g for $\text{La}_{65}\text{Co}_{25}\text{Al}_{10}$ MG after cooling from different T_a values. We used a Flash-DSC with a heating rate of 500 K/s to determine T_g ⁵⁶ and avoid overlap between the polymorphous transition and the glass transition (supplementary material Fig. S5). Such overlap could occur at lower heating rates in the conventional DSC. The data in Fig. 3 show a linear relation between T_β and T_g . Therefore, the enhanced T_β in PT-MGs can be attributed to the higher T_g . This relation is also consistent with the coupling model and some

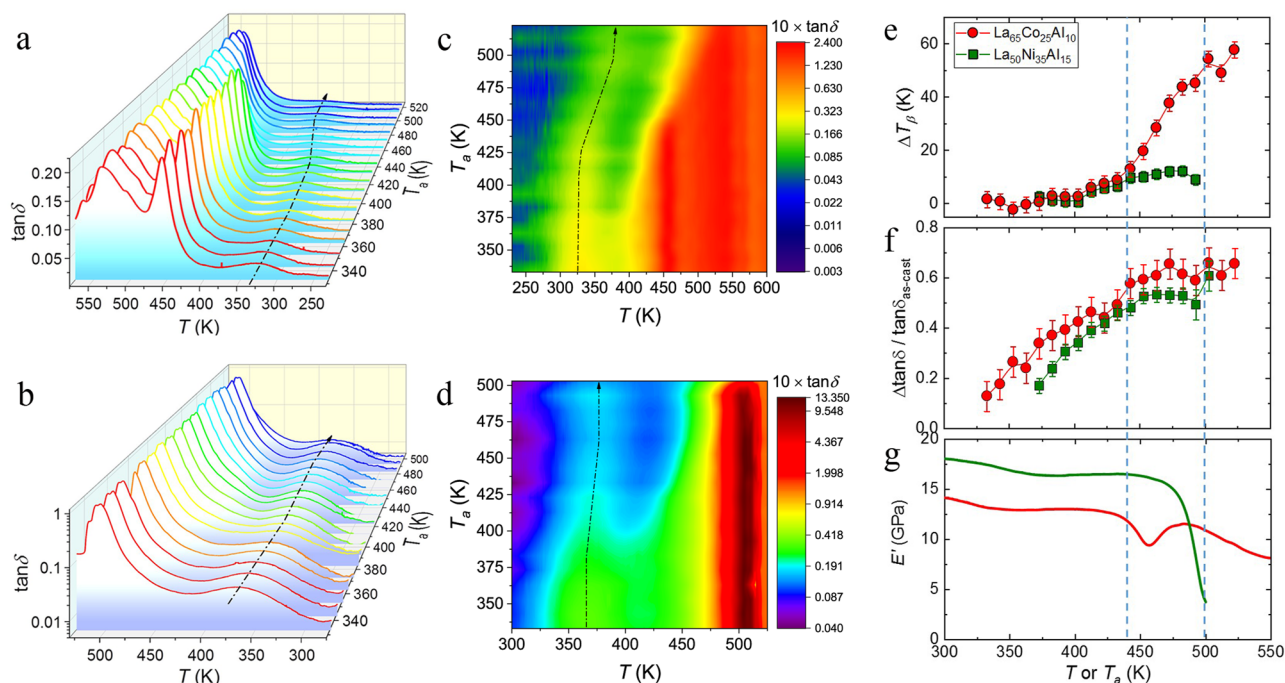


FIG. 2. Temperature dependence of damping factor $\tan \delta$ for heat-treated $\text{La}_{65}\text{Co}_{25}\text{Al}_{10}$ MG [top column (a) and -(b)] and $\text{La}_{50}\text{Ni}_{35}\text{Al}_{15}$ MG [bottom column (c) and -(d)] at different T_a (1 Hz), respectively. The position (e) and intensity (f) of the β relaxation peak evolve with T_a for the two MGs. (g) Temperature dependence of storage modulus E' for the two MGs, measured with a frequency of 1 Hz.

previous experimental results,^{26,27,57} where the temperatures of the β and α relaxations are always connected and a change of one would influence the other.

In situ, high-energy XRD experiments were performed on the as-prepared $\text{La}_{65}\text{Co}_{25}\text{Al}_{10}$ MG at temperatures from room temperature to 600 K (see Methods for details). Figure 4(a) shows the

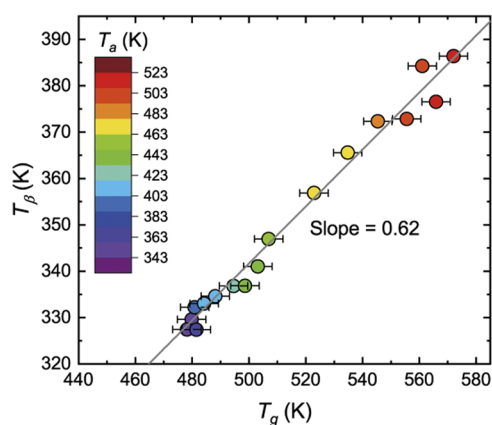


FIG. 3. Relation between the glass transition temperature T_g and the characteristic temperature of β relaxation T_β for the $\text{La}_{65}\text{Co}_{25}\text{Al}_{10}$ MGs, which are cooled from different T_a . Here, the glass transition temperature T_g is measured by Flash-DSC at a heating rate of 500 K/s.

structure factors $S(q)$ upon heating. We find that the $S(q)$ profile changes appreciably when heating above 450 K, which is approximately the temperature of the polyamorphous transition of MG. An additional diffuse scattering peak emerges around $q = 4.46 \text{ 1/\AA}$. As demonstrated by previous work, the $S(q)$ profile does not result from Bragg diffraction peaks caused by crystallization, but due to the transition to a more ordered amorphous phase.^{46,47} Meanwhile, above 450 K, the peak intensities of the second, third, and fourth maxima of $S(q)$ are all enhanced, and the profile of these peaks becomes narrower, implying an enhanced ordering of amorphous structures.

To more clearly show the structural evolution of the $\text{La}_{65}\text{Co}_{25}\text{Al}_{10}$ MG during heating, the reduced pair-correlation function $G(r)$ in real space is obtained by Fourier transforming $S(q)$ from the reciprocal space, as shown in Fig. 4(b). One can see that the oscillation of $G(r)$ at a temperature below 450 K dampens quickly for $r > 12 \text{ \AA}$, while it shows obvious enhancement at a temperature above 450 K, which extends over 20 \AA . This reveals that a more ordered amorphous structure is formed by a polyamorphous transformation. Pronounced changes are observed in $G(r)$ at the r range 5–17 \AA , which is identified as a typical structural feature associated with medium-range orders (MROs). Our results are consistent with previous studies showing that PT-MG has structural ordering at larger length scales, although it is still amorphous.^{46,47,49,51,53}

It is interesting to note that the position of the first maximum and the features for $r < 5 \text{ \AA}$ of $G(r)$ show negligible changes over the entire studied temperature range, as shown in Fig. 4(b) and a

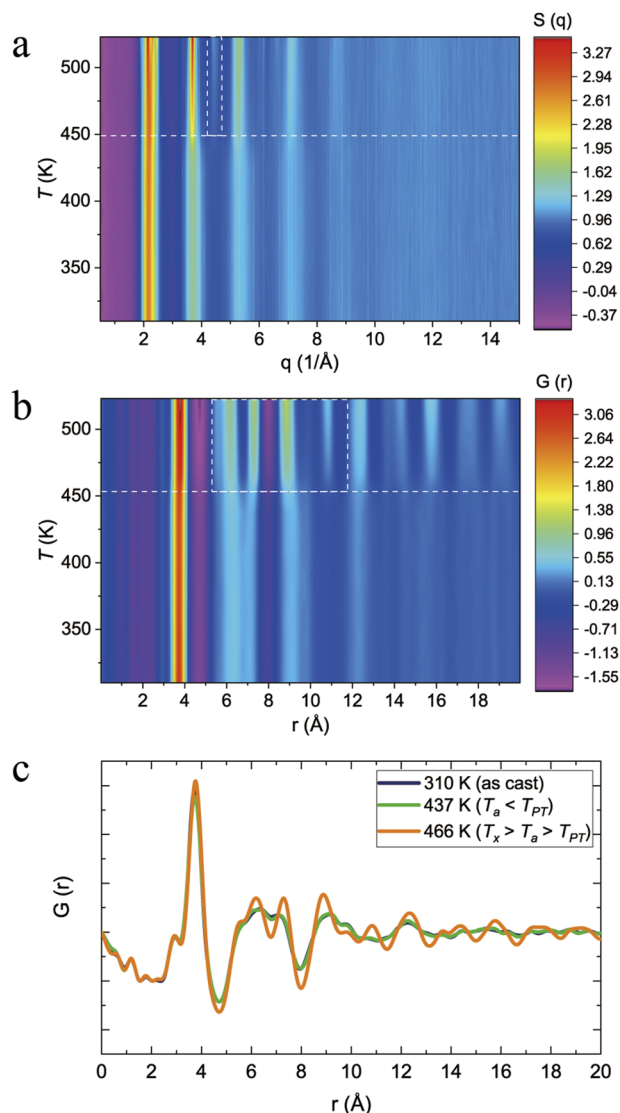


FIG. 4. Temperature dependence of the structural factor $S(q)$ (a) and the pair-correlation function $G(r)$ (b) for $\text{La}_{65}\text{Co}_{25}\text{Al}_{10}$ MG during heating, with a heating rate of 10 K/min. (c) Two representative pair-correlation functions at different temperatures (437 and 466 K) were selected to compare with the as-cast one (310 K), to illustrate the different effects of physical aging and polyamorphous transition on the structure.

selected plot in Fig. 4(c). Thus, the short-range order (SRO) of MG changes little over the polyamorphous transition.

It is clear from the above analysis that the polyamorphous transition mainly involves changes in MROs. Hence, the abrupt large increase in T_β (and T_g) in $\text{La}_{65}\text{Co}_{25}\text{Al}_{10}$ [Fig. 2(e)] can be attributed to the ordering of MROs. This implies that the MROs account mostly for the global stiffening of the glass (which leads to enhanced levels of both T_g and T_β). On the other hand, the intensity of the β relaxation peak shows no sudden change upon the polyamorphous transition [Fig. 2(f)]. This indicates that the magnitude of

β relaxation is dominated by the changes in SROs introduced through aging, not by the MROs. As such, the effects of MROs and SROs on β relaxations can be unambiguously separated in the polyamorphous system.

Molecular dynamics simulations revealed that cooperative, string-like atomic motions are the structural rearrangements governing the β relaxation in MGs. The string-like motions are related to the cage-breaking ability from confinements of the nearest neighbors.³¹ A more detailed study showed that the string-like motions involve atomic rattling in nearest neighboring cages and cage-breaking events. The β relaxation, which corresponds to string-like motions, must be a sequentially activated process. One atom jumps away and leaves a vacancy-like free site, and one nearby atom jumps to the free site, and the process is repeated. In this connection, SRO is the foremost factor that influences the cage-breaking event and the formation of string-like motions. Hence, our findings can be interpreted in this microscopic picture and provide evidence for the simulations from a structural perspective.

Finally, the recognition of the difference between the influences of SRO and MRO might have implications for some longstanding issues about β relaxation. In particular, it is puzzling that β relaxations depend crucially on the chemical composition of the materials^{7,20} but can be less tuned by physical methods such as annealing or cooling conditions.^{19,20,58} This might be understood by considering that chemical compositions can modify the SROs more readily, while physical methods such as annealing are less effective in changing SROs, but affect MROs more. This work represents a step forward in establishing the structure–dynamics relation, the ultimate goal of glassy physics.

SUPPLEMENTARY MATERIAL

This [supplementary material](#) provides the details of the experiments, including sample preparation, heat treatment procedures, structure characterizations, dynamical mechanical spectroscopy, and calorimetry measurement.

ACKNOWLEDGMENTS

The authors acknowledge DESY (Hamburg, Germany), a member of the Helmholtz Association (HGF), for the provision of experimental facilities. Parts of this research were carried out at PETRA III using beamline P02.1. Beamtime was allocated for the proposal (Grant No. I-20200462). This work was supported by China's Youth Thousand Talents Program and the Fundamental Research Funds for the Central Universities (Grant No. 2018KFYXKJC009).

AUTHOR DECLARATIONS

Conflict of Interest

The authors have no conflicts to disclose.

Author Contributions

Q.Y. and S.W. contributed equally to this work.

Qun Yang: Data curation (equal); Investigation (equal); Validation (equal); Visualization (equal); Writing – original draft (equal); Writing – review & editing (equal). **Shuai Wei:** Data curation

(equal); Funding acquisition (equal); Methodology (equal). **Yang Yu:** Data curation (equal); Methodology (equal). **Hui-Ru Zhang:** Data curation (equal); Investigation (equal). **Liang Gao:** Data curation (equal); Validation (equal). **Qing-Zhou Bu:** Data curation (equal); Validation (equal). **Narges Amini:** Data curation (equal). **Yu-Dong Cheng:** Data curation (equal); Validation (equal). **Fan Yang:** Data curation (equal); Funding acquisition (equal); Investigation (equal); Methodology (equal); Resources (equal). **Alexander Schoekel:** Data curation (equal); Investigation (equal). **Hai-Bin Yu:** Conceptualization (equal); Data curation (equal); Funding acquisition (equal); Investigation (equal); Methodology (equal); Resources (equal); Supervision (equal); Validation (equal); Visualization (equal); Writing – original draft (equal); Writing – review & editing (equal).

DATA AVAILABILITY

The data that support the findings of this study are available from the corresponding author upon reasonable request.

REFERENCES

- 1 Y. Yang, J. Zhou, F. Zhu, Y. Yuan, D. J. Chang, D. S. Kim, M. Pham, A. Rana, X. Tian, Y. Yao, S. J. Osher, A. K. Schmid, L. Hu, P. Ercius, and J. Miao, "Determining the three-dimensional atomic structure of an amorphous solid," *Nature* **592**, 60 (2021).
- 2 K. L. Ngai, *Relaxation and Diffusion in Complex Systems* (Springer, New York, 2011).
- 3 L. Berthier and M. D. Ediger, "Facets of glass physics," *Phys. Today* **69**(1), 40 (2016).
- 4 A. Zaccone, "Relaxation and vibrational properties in metal alloys and other disordered systems," *J. Phys.: Condens. Matter* **32**, 203001 (2020).
- 5 B. Ruta, E. Pineda, and Z. Evenson, "Relaxation processes and physical aging in metallic glasses," *J. Phys.: Condens. Matter* **29**, 503002 (2017).
- 6 B. Ruta, S. Hechler, N. Neuber, D. Orsi, L. Cristofolini, O. Gross, B. Bochtler, M. Frey, A. Kuball, S. S. Riegler, M. Stolpe, Z. Evenson, C. Gutt, F. Westermeier, R. Busch, and I. Gallino, "Wave-vector dependence of the dynamics in supercooled metallic liquids," *Phys. Rev. Lett.* **125**, 055701 (2020).
- 7 W. H. Wang, "Dynamic relaxations and relaxation-property relationships in metallic glasses," *Prog. Mater. Sci.* **106**, 100561 (2019).
- 8 C. Gainaru, H. Nelson, J. Huebinger, M. Grabenbauer, and R. Böhmer, "Suppression of orientational correlations in the viscous-liquid state of hyperquenched pressure-densified glycerol," *Phys. Rev. Lett.* **125**, 065503 (2020).
- 9 K. Geirhos, P. Lunkenheimer, and A. Loidl, "Johari-Goldstein relaxation far below T_g : Experimental evidence for the gardner transition in structural glasses?," *Phys. Rev. Lett.* **120**, 085705 (2018).
- 10 M. Vogel and E. Rössler, "On the nature of slow β -process in simple glass formers: A 2H NMR study," *J. Phys. Chem. B* **104**, 4285 (2000).
- 11 M. Vogel, P. Medick, and E. A. Rössler, in *Annual Reports on NMR Spectroscopy*, edited by G. A. Webb (Academic Press, 2005), p. 231.
- 12 A. Kudlik, C. Tschirwitz, T. Blochowicz, S. Benkhof, and E. Rössler, "Slow secondary relaxation in simple glass formers," *J. Non-Cryst. Solids* **235–237**, 406 (1998).
- 13 A. Döb, M. Paluch, H. Sillescu, and G. Hinze, "From strong to fragile glass formers: Secondary relaxation in polyalcohols," *Phys. Rev. Lett.* **88**, 095701 (2002).
- 14 F. Micciche, V. Ramakrishnan, and T. L. Hoeks, "The effect of molecular structure on the secondary transitions and their influence on the decoloration kinetics of photochromic dyes in co-polycarbonates," *J. Polym. Sci., Part B: Polym. Phys.* **54**, 1593 (2016).
- 15 R. Casalini and C. M. Roland, "Aging of the secondary relaxation to probe structural relaxation in the glassy state," *Phys. Rev. Lett.* **102**, 035701 (2009).
- 16 S. A. Lusceac, C. Gainaru, M. Vogel, C. Koplin, P. Medick, and E. A. Rössler, "Secondary relaxation processes in polybutadiene studied by 2H nuclear magnetic resonance and high-precision dielectric spectroscopy," *Macromolecules* **38**, 5625 (2005).
- 17 Z. Wojnarowska, M. Musiał, S. Cheng, E. Drockenmüller, and M. Paluch, "Fast secondary dynamics for enhanced charge transport in polymerized ionic liquids," *Phys. Rev. E* **101**, 032606 (2020).
- 18 M. Paluch, Z. Wojnarowska, and S. Hensel-Bielowka, "Heterogeneous dynamics of prototypical ionic glass CKN monitored by physical aging," *Phys. Rev. Lett.* **110**, 015702 (2013).
- 19 J. C. Qiao, Q. Wang, J. M. Pelletier, H. Kato, R. Casalini, D. Crespo, E. Pineda, Y. Yao, and Y. Yang, "Structural heterogeneities and mechanical behavior of amorphous alloys," *Prog. Mater. Sci.* **104**, 250 (2019).
- 20 H. B. Yu, W. H. Wang, H. Y. Bai, and K. Samwer, "The β -relaxation in metallic glasses," *Natl. Sci. Rev.* **1**, 429 (2014).
- 21 S.-X. Peng, Y. Cheng, J. Pries, S. Wei, H.-B. Yu, and M. Wuttig, "Uncovering β -relaxations in amorphous phase-change materials," *Sci. Adv.* **6**, eaay6726 (2020).
- 22 Q. Yang, C.-Q. Pei, H.-B. Yu, and T. Feng, "Metallic nanoglasses with promoted β -relaxation and tensile plasticity," *Nano Lett.* **21**, 6051 (2021).
- 23 N. He, L. Song, W. Xu, J. Huo, J.-Q. Wang, and R.-W. Li, "The evolution of relaxation modes during isothermal annealing and its influence on properties of Fe-based metallic glass," *J. Non-Cryst. Solids* **509**, 95 (2019).
- 24 C. Qian, Z.-G. Fan, W.-W. Zheng, R.-X. Bei, T.-W. Zhu, S.-W. Liu, Z.-G. Chi, M. P. Aldred, X.-D. Chen, Y. Zhang, and J.-R. Xu, "A facile strategy for non-fluorinated intrinsic low- k and low-loss dielectric polymers: Valid exploitation of secondary relaxation behaviors," *Chin. J. Polym. Sci.* **38**, 213 (2020).
- 25 S. Capaccioli, M. Paluch, D. Prevosto, L.-M. Wang, and K. L. Ngai, "Many-body nature of relaxation processes in glass-forming systems," *J. Phys. Chem. Lett.* **3**, 735 (2012).
- 26 K. L. Ngai and S. Capaccioli, "Relation between the activation energy of the Johari-Goldstein β relaxation and T_g of glass formers," *Phys. Rev. E* **69**, 031501 (2004).
- 27 Z. Wang and W.-H. Wang, "Flow units as dynamic defects in metallic glassy materials," *Natl. Sci. Rev.* **6**, 304 (2018).
- 28 K. L. Ngai, "Microscopic understanding of the Johari-Goldstein β relaxation gained from nuclear γ -resonance time-domain-interferometry experiments," *Phys. Rev. E* **104**, 015103 (2021).
- 29 X. D. Wang, J. Zhang, T. D. Xu, Q. Yu, Q. P. Cao, D. X. Zhang, and J. Z. Jiang, "Structural signature of β -relaxation in La-based metallic glasses," *J. Phys. Chem. Lett.* **9**, 4308 (2018).
- 30 B. Micko, C. Tschirwitz, and E. A. Rössler, "Secondary relaxation processes in binary glass formers: Emergence of 'islands of rigidity'," *J. Chem. Phys.* **138**, 154501 (2013).
- 31 H.-B. Yu, R. Richert, and K. Samwer, "Structural rearrangements governing Johari-Goldstein relaxations in metallic glasses," *Sci. Adv.* **3**, e1701577 (2017).
- 32 D. Bedorf and K. Samwer, "Length scale effects on relaxations in metallic glasses," *J. Non-Cryst. Solids* **356**, 340 (2010).
- 33 S. T. Liu, Z. Wang, H. L. Peng, H. B. Yu, and W. H. Wang, "The activation energy and volume of flow units of metallic glasses," *Scr. Mater.* **67**, 9 (2012).
- 34 H. B. Yu, W. H. Wang, H. Y. Bai, Y. Wu, and M. W. Chen, "Relating activation of shear transformation zones to β relaxations in metallic glasses," *Phys. Rev. B* **81**, 220201 (2010).
- 35 D. P. Wang, J. C. Qiao, and C. T. Liu, "Relating structural heterogeneity to β relaxation processes in metallic glasses," *Mater. Res. Lett.* **7**, 305 (2019).
- 36 M. Saito, R. Masuda, Y. Yoda, and M. Seto, "Synchrotron radiation-based quasi-elastic scattering using time-domain interferometry with multi-line gamma rays," *Sci. Rep.* **7**, 12558 (2017).
- 37 M. Saito, M. Kurokuzu, Y. Yoda, and M. Seto, "Microscopic observation of hidden Johari-Goldstein- β process in glycerol," *Phys. Rev. E* **105**, L012605 (2022).
- 38 M. Saito, S. Kitao, Y. Kobayashi, M. Kurokuzu, Y. Yoda, and M. Seto, "Slow processes in supercooled o-terphenyl: Relaxation and decoupling," *Phys. Rev. Lett.* **109**, 115705 (2012).
- 39 T. Kanaya, R. Inoue, M. Saito, M. Seto, and Y. Yoda, "Relaxation transition in glass-forming polybutadiene as revealed by nuclear resonance X-ray scattering," *J. Chem. Phys.* **140**, 144906 (2014).

- ⁴⁰F. Caporaletti, S. Capaccioli, S. Valenti, M. Mikolasek, A. I. Chumakov, and G. Monaco, "Experimental evidence of mosaic structure in strongly supercooled molecular liquids," *Nat. Commun.* **12**, 1867 (2021).
- ⁴¹F. Caporaletti, S. Capaccioli, S. Valenti, M. Mikolasek, A. I. Chumakov, and G. Monaco, "A microscopic look at the Johari-Goldstein relaxation in a hydrogen-bonded glass-former," *Sci. Rep.* **9**, 14319 (2019).
- ⁴²L. Henry, M. Mezouar, G. Garbarino, D. Sifré, G. Weck, and F. Datchi, "Liquid-liquid transition and critical point in sulfur," *Nature* **584**, 382 (2020).
- ⁴³A. Zhang, Y. Jin, T. Liu, R. B. Stephens, and Z. Fakhraai, "Polyamorphism of vapor-deposited amorphous selenium in response to light," *Proc. Natl. Acad. Sci. U. S. A.* **117**, 24076 (2020).
- ⁴⁴P. Zalden, F. Quirin, M. Schumacher, J. Siegel, S. Wei, A. Koc, M. Nicoul, M. Trigo, P. Andreasson, H. Enquist, M. J. Shu, T. Pardini, M. Chollet, D. Zhu, H. Lemke, I. Ronneberger, J. Larsson, A. M. Lindenberg, H. E. Fischer, S. Hau-Riege, D. A. Reis, R. Mazzarello, M. Wuttig, and K. Sokolowski-Tinten, "Femtosecond x-ray diffraction reveals a liquid-liquid phase transition in phase-change materials," *Science* **364**, 1062 (2019).
- ⁴⁵H. Tanaka, "Liquid-liquid transition and polyamorphism," *J. Chem. Phys.* **153**, 130901 (2020).
- ⁴⁶H. Lou, Z. Zeng, F. Zhang, S. Chen, P. Luo, X. Chen, Y. Ren, V. B. Prakapenka, C. Prescher, X. Zuo, T. Li, J. Wen, W.-H. Wang, H. Sheng, and Q. Zeng, "Two-way tuning of structural order in metallic glasses," *Nat. Commun.* **11**, 314 (2020).
- ⁴⁷J. Shen, Z. Lu, J. Q. Wang, S. Lan, F. Zhang, A. Hirata, M. W. Chen, X. L. Wang, P. Wen, Y. H. Sun, H. Y. Bai, and W. H. Wang, "Metallic glacial glass formation by a first-order liquid-liquid transition," *J. Phys. Chem. Lett.* **11**, 6718 (2020).
- ⁴⁸K.-i. Murata and H. Tanaka, "Link between molecular mobility and order parameter during liquid-liquid transition of a molecular liquid," *Proc. Natl. Acad. Sci. U. S. A.* **116**, 7176 (2019).
- ⁴⁹S. Lan, Y. Ren, X. Y. Wei, B. Wang, E. P. Gilbert, T. Shibayama, S. Watanabe, M. Ohnuma, and X.-L. Wang, "Hidden amorphous phase and reentrant supercooled liquid in Pd-Ni-P metallic glasses," *Nat. Commun.* **8**, 14679 (2017).
- ⁵⁰J. P. Gabriel, B. Riechers, E. Thoms, A. Guiseppi-Elie, M. D. Ediger, and R. Richert, "Polyamorphism in vapor-deposited 2-methyltetrahydrofuran: A broadband dielectric relaxation study," *J. Chem. Phys.* **154**, 024502 (2021).
- ⁵¹Q. Du, X. Liu, H. Fan, Q. Zeng, Y. Wu, H. Wang, D. Chatterjee, Y. Ren, Y. Ke, P. M. Voyles, Z. Lu, and E. Ma, "Reentrant glass transition leading to ultrastable metallic glass," *Mater. Today* **34**, 66 (2020).
- ⁵²M. S. Beasley, B. J. Kasting, M. E. Tracy, A. Guiseppi-Elie, R. Richert, and M. D. Ediger, "Physical vapor deposition of a polyamorphic system: Triphenyl phosphite," *J. Chem. Phys.* **153**, 124511 (2020).
- ⁵³H. Luan, X. Zhang, H. Ding, F. Zhang, J. H. Luan, Z. B. Jiao, Y.-C. Yang, H. Bu, R. Wang, J. Gu, C. Shao, Q. Yu, Y. Shao, Q. Zeng, N. Chen, C. T. Liu, and K.-F. Yao, "High-entropy induced a glass-to-glass transition in a metallic glass," *Nat. Commun.* **13**, 2183 (2022).
- ⁵⁴P. Luo, C. R. Cao, F. Zhu, Y. M. Lv, Y. H. Liu, P. Wen, H. Y. Bai, G. Vaughan, M. di Michiel, B. Ruta, and W. H. Wang, "Ultrastable metallic glasses formed on cold substrates," *Nat. Commun.* **9**, 1389 (2018).
- ⁵⁵M. D. Ediger, "Perspective: Highly stable vapor-deposited glasses," *J. Chem. Phys.* **147**, 210901 (2017).
- ⁵⁶Q. Yang, S.-X. Peng, Z. Wang, and H.-B. Yu, "Shadow glass transition as a thermodynamic signature of β relaxation in hyper-quenched metallic glasses," *Natl. Sci. Rev.* **7**, 1896 (2020).
- ⁵⁷K. L. Ngai, "Relation between some secondary relaxations and the α relaxations in glass-forming materials according to the coupling model," *J. Chem. Phys.* **109**, 6982 (1998).
- ⁵⁸L. Z. Zhao, W. H. Wang, and H. Y. Bai, "Modulation of β -relaxation by modifying structural configurations in metallic glasses," *J. Non-Cryst. Solids* **405**, 207 (2014).